Polymer Chemistry

Synthesis and visualization of molecular brush-*on*-brush based hierarchically branched structures

Journal:	*Polymer Chemistry*
Manuscript ID	PY-COM-07-2019-001075.R1
Article Type:	Communication
Date Submitted by the Author:	04-Sep-2019
Complete List of Authors:	Fu, Xiaowei; Yale University, Chemical & Environmental Engineering; Sichuan University Guo, Zi-Hao; Yale University, Chemical & Environmental Engineering; South China University of Technology Le, An; Yale University, Chemical & Environmental Engineering Lei, Jingxin; Sichuan University, Zhong, Mingjiang; Yale University, Chemical & Environmental Engineering

COMMUNICATION

Synthesis and visualization of molecular brush-*on*-brush based hierarchically branched structures

Received 00th January 20xx,
Accepted 00th January 20xx

DOI: 10.1039/x0xx00000x

Xiaowei Fu,[a,b] Zi-Hao Guo,[a,c] An N. Le,[a] Jingxin Lei,[b] and Mingjiang Zhong*,[a]

An atom transfer radical polymerization-based sequential "graft-from" approach was developed to synthesize molecular brush-*on*-brush (MBoB)-based hierarchically branched polymers with readily tunable backbone grafting density, lengths of backbone and primary/secondary side chains, and monomer type. The hierarchically branched structure was visualized, and the stability of the giant MBoB macromolecules was studied by atomic force microscopy. The robust approach enabled the versatile combination of chemical functionality and MBoB structure.

Hierarchically branched structures, derived from covalent or supramolecular multi-scale assembly of molecular building blocks, could play a critical role in the diverse functions of biological systems[1-3]. One representative example is the supramolecular brush-*on*-brush (BoB) structure that captures the nature of cartilage-specific aggrecan aggregates. These aggregates comprise aggrecan monomers non-covalently attached to hyaluronan as the backbone. Core protein and glycosaminoglycan in the aggrecan monomers serve as primary and secondary side chains, respectively.[4-6] The structure-enabled physiological properties observed in aggrecan aggregates have motivated chemists to develop strategies for the synthesis of molecular brush architectures.[7-11] While conventional molecular brushes have demonstrated potential applications in photonic crystals[12-15], bio-lubrication[9,16], super-soft elastomers[17,18], and biomedical engineering[19-21], synthesis of hierarchically branched single molecules that mimic the supramolecular aggrecan aggregate structure, i.e., a molecular BoB (MBoB) architecture, have rarely been reported.[22-24] Controlled synthesis of MBoBs with readily tunable structural parameters and diverse functional groups and subsequent development of their structure-property relationships would shed light on the design and optimization of bioinspired and biomimetic materials.

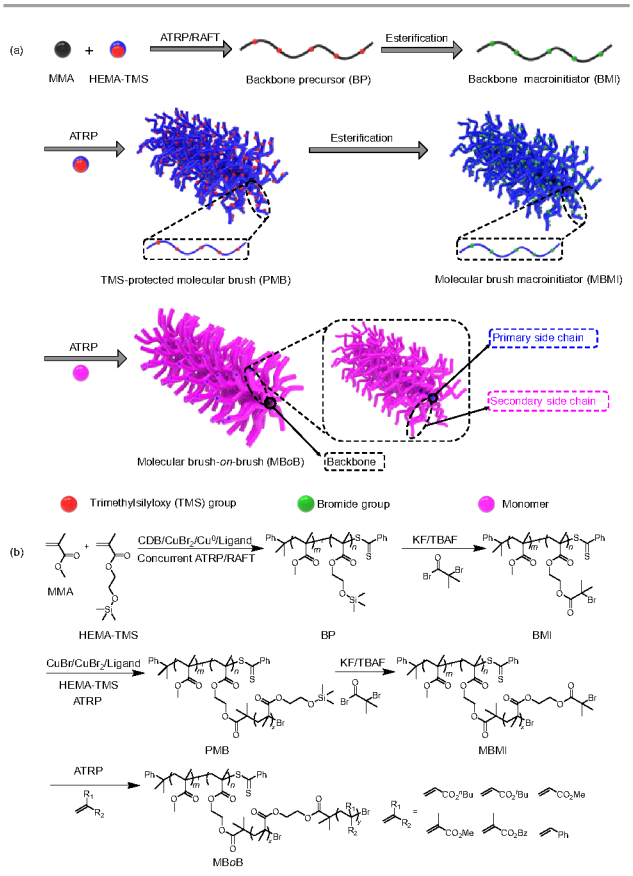

Scheme 1. (a) Hierarchical architecture and (b) synthetic route to MBoBs.

In an effort to obtain the MBoBs, an atom transfer radical polymerization (ATRP)-based sequential "graft-from"[25,26] approach was developed in this work (Scheme 1). Scalable synthesis of MBoBs with tunable backbone grafting density and lengths of both the backbone and primary/secondary side

[a] *Department of Chemical and Environmental Engineering, Yale University, New Haven, Connecticut 06520, United States. Email: mingjiang.zhong@yale.edu*
[b] *State Key Laboratory of Polymer Materials Engineering, Polymer Research Institute of Sichuan University, Chengdu 610065, China.*
[c] *South China Advanced Institute for Soft Matter Science and Technology, School of Molecular Science and Engineering, South China University of Technology, Guangzhou 510640, China*
Electronic Supplementary Information (ESI) available: Synthetic and analytic details. See DOI: 10.1039/x0xx00000x

chains were enabled by a facile and versatile "grafting-from" strategy. Atomic force microscopy (AFM) was employed to confirm the structure of the hierarchically branched single molecules, and the stability of the synthesized giant molecules was evaluated on a mica substrate.

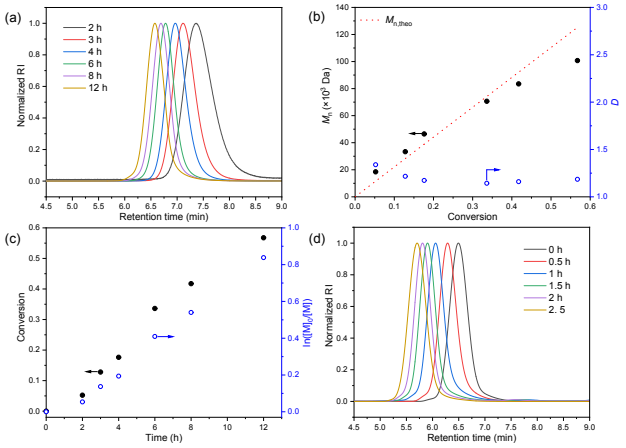

Figure 1. (a) GPC traces, (b) M_n and $Đ$ versus monomer conversion, and (c) kinetic data in the polymerization for the preparation of BP-1; (d) GPC traces in the polymerization for the PMB-2 preparation.

Concurrent ATRP/reversible addition-fragmentation transfer (RAFT) polymerization[27,28] was employed to prepare copolymers consisting of methyl methacrylate (MMA) and 2-(trimethylsilyloxy)ethyl methacrylate (HEMA-TMS) as the backbone precursors (BPs). This unusual polymerization technique is able to synthesize polymers with ultrahigh molecular weights in a well-controlled manner due to its thermal-initiator-free initiation and two synergistically-cooperating reversible-deactivation mechanisms. BPs with various monomer ratios were labeled as BP-*p* (Table S1, *p* = 1, 2), where *p* is used to represent the sample number in this report. Cumyl dithiobenzoate (CDB) served as both a chain-transfer agent in the RAFT process and an initiator of ATRP that can be activated by the *in-situ* (re)generated Cu^{I}/tris[2-(dimethylamino)ethyl]amine (Me_6TREN), enabling the synthesis of copolymers with ultra-high degree of polymerization (DP > 1000) and relatively low dispersity ($Đ$ < 1.3).

Figure 1a–c presents the polymerization results for BP-1. Controlled polymerization was confirmed by the narrow molecular weight distribution (Figure 1a,b) that was evaluated by gel permeation chromatography (GPC), a good agreement between experimental ($M_{n,GPC}$) and theoretical ($M_{n,theo}$) number-average molecular weights determined by monomer conversions (Figure 1b), and the pseudo-first-order kinetics (Figure 1c). The polymerization was stopped in 12 h with a conversion of 56.7%, determined by ^{1}H nuclear magnetic resonance (^{1}H-NMR) spectroscopy, offering a composition of P(MMA_{1021}-*r*-HEMA-TMS_{113}) ($M_{n,GPC}$ = 1.22 × 10^5 Da, $Đ$ = 1.18).

The one-pot deprotection and esterification at the trimethylsilyloxy (TMS)-protected sites of the BPs were conducted to obtain the backbone macroinitiators (BMIs) for the subsequent integration of primary side chains. The BMIs with various compositions were labeled as BMI-*p* (Table S2, *p* = 1, 2). A quantitative transformation of HEMA-TMS derived repeating units to (2-bromoisobutyryloxy)ethyl methacrylate (BIBEM) [18,29] counterparts was verified by the absence of TMS protons (0.14 ppm) and the presence of methyl protons (1.98 ppm) adjacent to the bromine atom of BIBEM in the ^{1}H-NMR spectrum (Figure S5).

ATRP of HEMA-TMS in the presence of BMIs resulted in the formation of TMS-protected molecular brushes (PMBs) containing the primary side chain precursor of MB*o*Bs (Table S4). For instance, PMB-2 with primary side chains of DP = 64 ($M_{n,GPC}$ = 5.98 × 10^5 Da, $Đ$ = 1.1) was synthesized from BMI-1 (Figure 1d). The site-specific initiation in the graft-from experiment was demonstrated by the clear shift of GPC traces from the BMI (at 0 h), as well as the absence of low molecular weight polymers (Figure 1d). Polymerizations with low monomer conversion (< 10%) and high monomer dilution were conducted so that inter-brush coupling was suppressed, as evidenced by the absence of high molecular weight polymers.[30,31] Corresponding molecular brush macroinitiators (MBMIs) derived from PMBs were prepared through similar one-pot deprotection and esterification conditions that were employed in the preparation of BMIs (Table S5). The large discrepancy between $M_{n,theo}$ and $M_{n,GPC}$ of the molecular brushes could be attributed to their small hydrodynamic volumes resulting from their compact molecular conformation, compared to their linear counterparts of the same molecular weights.

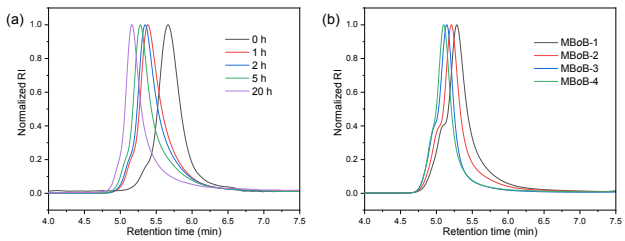

Figure 2. (a) GPC traces in the polymerization for the MB*o*B-5 preparation; (b) GPC traces of MB*o*Bs with various DPs of secondary side chains.

MB*o*Bs were prepared through another round of ATRP-mediated "graft-from" reactions using MBMI as the initiator. To minimize intermolecular coupling, the ATRP polymerization was also terminated at low conversions (< 10%) with monomer-diluted reaction conditions (nearly bulk polymerization). For example, the secondary side chains of poly(*n*-butyl acrylate) (P*n*BA) were installed in the presence of MBMI-2, and GPC traces clearly shifted towards the high molecular weight regime with increased reaction time (Figure 2a).

Hierarchically-branched MB*o*B architectures with varied backbone DPs and grafting density and lengths of primary/secondary side chains were readily prepared, and the MB*o*B samples with various compositions, i.e., MB*o*B-*p* (*p* = 1–15), are summarized in Table 1. MB*o*Bs with various lengths of

Table 1. Structural parameters of MBoBs.

Samples	m^a	n^a	x^a	y (M)^a	$M_{n,GPC}$ (×10^5 Da)^b	$M_{n,theo}$ (×10^6 Da)	$Đ^b$
MB*o*B-1	1021	113	33	18 (*n*BA)	10.73	9.77	1.32
MB*o*B-2	1021	113	33	22 (*n*BA)	14.49	11.68	1.16
MB*o*B-3	1021	113	33	54 (*n*BA)	16.42	26.98	1.13
MB*o*B-4	1021	113	33	63 (*n*BA)	18.26	31.28	1.11
MB*o*B-5	1021	113	64	22 (*n*BA)	14.85	22.54	1.14
MB*o*B-6	1021	113	64	26 (*n*BA)	16.32	26.25	1.15
MB*o*B-7	1021	113	64	36 (*n*BA)	18.27	35.52	1.08
MB*o*B-8	1021	113	64	46 (*n*BA)	20.29	44.79	1.07
MB*o*B-9	1152	12	30	33 (*t*BA)	4.46	1.81	1.11
MB*o*B-10	1152	12	30	53 (*t*BA)	5.54	2.73	1.13
MB*o*B-11	1152	12	30	92 (MA)	5.08	3.07	1.17
MB*o*B-12	1152	12	30	38 (BzMA)	4.72	2.62	1.15
MB*o*B-13	1152	12	30	56 (MMA)	5.12	2.23	1.23
MB*o*B-14	1152	12	30	14 (St)	3.2	0.74	1.14
MB*o*B-15	1152	12	30	53 (AA)	ND	1.59	ND

[a] *m* and *n* are the numbers of units of MMA and BIBEM, respectively, in the backbone; *x* and *y* are the DPs of the primary and secondary side chains, respectively; M represents the monomer used in the synthesis of the secondary side chains; *n*BA = *n*-butyl acrylate, *t*BA = *tert*-butyl acrylate, MA = methyl acrylate, BzMA = benzyl methacrylate, St = styrene, AA = acrylic acid. [b] $M_{n,GPC}$ and *Đ* were obtained from THF GPC, calibrated with linear polystyrene standards.

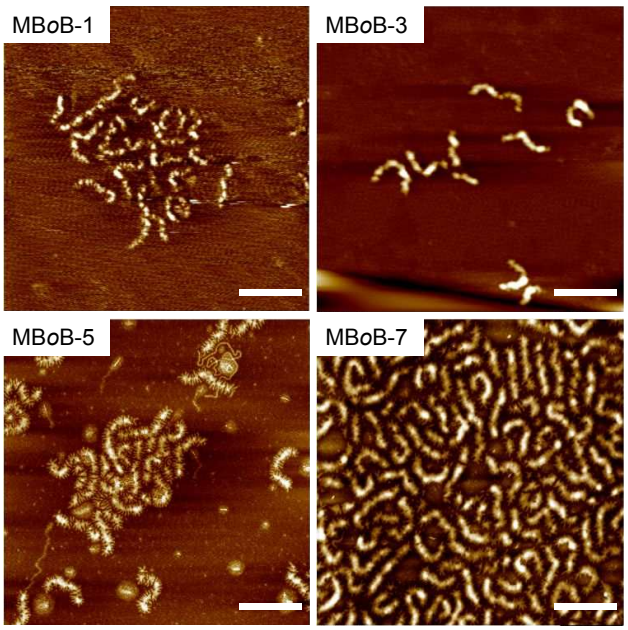

Figure 3. AFM height images of MB*o*Bs. The scale bars are 400 nm.

secondary side chains were prepared from the same MBMI-1, and only negligible intermolecular coupling (<10%), evidenced by the shoulder peaks in the GPC traces, was detected (Figure 2b). The $M_{n,GPC}$ shifted from 1.07 × 10^6 Da to 1.82 × 10^6 Da with increasing DPs of the secondary side chains from 18 to 63 (MB*o*Bs-1, 2, 3, 4). The absence of low molecular weight polymers indicated exclusive initiation from the MBMI. Compared to the MBMI samples, the MB*o*B samples showed an even larger discrepancy between $M_{n,theo}$ and $M_{n,GPC}$ as a result of the more compact molecular conformation, leading to drastically different hydrodynamic volumes between MB*o*Bs and the linear polystyrene GPC standards.

The morphologies of MB*o*Bs were imaged by AFM (Figure 3, Figure S35-39). An extended worm-like feature with clear hairy corona structures was observed in the majority of the MB*o*B samples. Increasing DPs of the secondary side chains from 18 to 54 yielded a thickened (width from 37 nm to 45 nm) and extended (contour length from 331 nm to 363 nm) worm-like morphology (Table S7). These AFM results indicated that the secondary side chains could simultaneously extend and thicken the primary side chains, further thickening and extending the worm-like morphology of the entire MB*o*Bs. A further increase in DP of the secondary side chains to 63 generated severe scission of the backbone upon spin-coating on mica substrates, possibly due to the tension along the backbone caused by the large steric repulsion of side chains on the surface (Figure S38).[32]

Interestingly, no apparent scission of the backbone was observed on mica substrates when the length of the primary side chains was extended to a DP of 64 while limiting the DPs of the secondary side chains up to 36 (e.g., MB*o*Bs-5,7, Table S7). This enhanced stability could be ascribed to the fact that the decrease in the thickness of side chain brushes, i.e., DPs of secondary side chains, resulted in reduced tension in MB*o*Bs even though side chain brushes were elongated. While keeping the same secondary side chains (DP = 22), increasing the DP of the

primary side chains from 33 to 64 significantly thickened the worm-like morphologies, from 45 nm to 69 nm, and extended the contour length slightly, from 336 nm to 352 nm (MB*o*Bs-2, 5).

To further demonstrate the versatility of the approach of sequential "graft-from" reactions toward MB*o*B architectures, MB*o*Bs with the secondary side chains of polyacrylate (MB*o*Bs-9, 10, 11), polymethacrylate (MB*o*Bs-12, 13), and polystyrene (MB*o*B-14) were synthesized with controlled molecular weights and low dispersity ($Đ$ < 1.2). An MB*o*B with secondary side chains of sodium acrylate was prepared by deprotection of *tert*-butyl groups of MB*o*B-10 and subsequent neutralization (MB*o*B-15, Figure S32). An MB*o*B with secondary side chains of poly(benzyl methacrylate)$_{38}$-*block*-poly(*tert*-butyl acrylate)$_{69}$ di-block copolymers was synthesized through further chain extension of MB*o*B-12 with secondary side chains of poly(benzyl methacrylate)$_{38}$, indicating the good fidelity of terminal bromide groups (Figure S33 and S34).

In summary, the hierarchically branched MB*o*Bs were synthesized via an ATRP-based sequential "graft-from" method. The worm-like morphologies of P*n*BA-based MB*o*Bs with clear hairy corona structures were visualized by AFM. The lengths of backbone and primary/secondary side chains as well as backbone grafting density were readily tuned through rationally varying the monomer conversion and comonomer ratio in the polymerization. The versatility of this approach toward MB*o*Bs was further corroborated by installing various homo- or block copolymers of *t*BA, MA, BzMA, St and sodium acrylate as the secondary side chains. Structure-property relationships of the synthesized MB*o*Bs are currently under investigation in our research group.

Conflicts of interest

The authors declare no conflict of interest.

Acknowledgements

X.F. is thankful for the financial support from the China Scholarship Council (CSC No. 201706240130) for the two-year visit at Yale University. A.N.L. acknowledges support from the National Science Foundation Graduate Research Fellowships. This work was also financially supported by Yale University Lab Setup Funds.

Notes and references

1 K. Matyjaszewski, *Science*, 2011, **333**, 1104-1105.
2 J.-F. Lutz, J.-M. Lehn, E. W. Meijer and K. Matyjaszewski, *Nature Reviews Materials*, 2016, **1**, 16024.
3 F. Li, M. Cao, Y. Feng, R. Liang, X. Fu and M. Zhong, *J. Am. Chem. Soc.*, 2019, **141**, 794-799.
4 C. Kiani, L. Chen, Y. J. Wu, A. J. Yee and B. B. Yang, *Cell Research*, 2002, **12**, 19-32.
5 A. G. Bajpayee and A. J. Grodzinsky, *Nature Reviews Rheumatology*, 2017, **13**, 183-193.
6 H.-Y. Lee, L. Han, P. J. Roughley, A. J. Grodzinsky and C. Ortiz, *Journal of Structural Biology*, 2013, **181**, 264-273.
7 Y. Xia, V. Adibnia, R. Huang, F. Murschel, J. Faivre, G. Xie, M. Olszewski, G. De Crescenzo, W. Qi, Z. He, R. Su, K. Matyjaszewski and X. Banquy, *Angew. Chem. Int. Edit.*, 2019, **58**, hyaluronan.
8 K. Lienkamp, L. Noé, M.-H. Breniaux, I. Lieberwirth, F. Groehn and G. Wegner, *Macromolecules*, 2007, **40**, 2486-2502.
9 G. Xie, M. R. Martinez, M. Olszewski, S. S. Sheiko and K. Matyjaszewski, *Biomacromolecules*, 2018, **20**, 27-54.
10 A. N. Le, R. Liang and M. Zhong, *Chemistry – A European Journal*, 2019, **25**, 8177-8189.
11 G. Zi-Hao, L. A. N., F. Xunda, C. Youngwoo, L. Bingqian, W. Danyu, W. Zhengyi, G. Yuwei, Z. Julia, L. Vince, O. C. O., J. J. A. and Z. Mingjiang, *Angew. Chem. Int. Edit.*, 2018, **57**, 8493-8497.
12 M. Vatankhah-Varnosfaderani, A. N. Keith, Y. Cong, H. Liang, M. Rosenthal, M. Sztucki, C. Clair, S. Magonov, D. A. Ivanov, A. V. Dobrynin and S. S. Sheiko, *Science*, 2018, **359**, 1509-1513.
13 Y. Xia, B. D. Olsen, J. A. Kornfield and R. H. Grubbs, *J. Am. Chem. Soc.*, 2009, **131**, 18525-18532.
14 S. Dong‐Po, L. Cheng, C. N. S., L. Xuemin, L. Jae‐Hwang and W. J. J., *Advanced Optical Materials*, 2015, **3**, 1169-1175.
15 G. M. Miyake, V. A. Piunova, R. A. Weitekamp and R. H. Grubbs, *Angew. Chem. Int. Edit.*, 2012, **51**, 11246-11248.
16 X. Banquy, J. Burdyńska, D. W. Lee, K. Matyjaszewski and J. Israelachvili, *J. Am. Chem. Soc.*, 2014, **136**, 6199-6202.
17 W. F. M. Daniel, J. Burdyńska, M. Vatankhah-Varnoosfaderani, K. Matyjaszewski, J. Paturej, M. Rubinstein, A. V. Dobrynin and S. S. Sheiko, *Nat. Mater.*, 2016, **15**, 183-189.
18 W. F. M. Daniel, G. Xie, M. Vatankhah Varnoosfaderani, J. Burdyńska, Q. Li, D. Nykypanchuk, O. Gang, K. Matyjaszewski and S. S. Sheiko, *Macromolecules*, 2017, **50**, 2103-2111.
19 L. Liao, J. Liu, E. C. Dreaden, S. W. Morton, K. E. Shopsowitz, P. T. Hammond and J. A. Johnson, *J. Am. Chem. Soc.*, 2014, **136**, 5896-5899.
20 S. S. Sheiko, M. H. Everhart, A. V. Dobrynin and M. Vatankhah-Varnosfaderani, *Science Robotics*, 2018, **3**.
21 H. Unsal, S. Onbulak, F. Calik, M. Er-Rafik, M. Schmutz, A. Sanyal and J. Rzayev, *Macromolecules*, 2017, **50**, 1342-1352.
22 Y. Chen, Z. Sun, H. Li, Y. Dai, Z. Hu, H. Huang, Y. Shi, Y. Li and Y. Chen, *ACS Macro Lett.*, 2019, **8**, 749-753.
23 T. Pelras, C. S. Mahon, Nonappa, O. Ikkala, A. H. Gröschel and M. Müllner, *J. Am. Chem. Soc.*, 2018, **140**, 12736-12740.
24 T. Krivorotova, R. Makuska, A. Naderi, P. M. Claesson and A. Dedinaite, *Eur. Polym. J.*, 2010, **46**, 171-180.
25 S. S. Sheiko, B. S. Sumerlin and K. Matyjaszewski, *Prog. Polym. Sci.*, 2008, **33**, 759-785.
26 B. Xu, C. Feng and X. Huang, *Nature Communications*, 2017, **8**, 333.
27 R. Nicolaÿ, Y. Kwak and K. Matyjaszewski, *Angew. Chem. Int. Edit.*, 2010, **49**, 541-544.
28 J. K. D. Mapas, T. Thomay, A. N. Cartwright, J. Ilavsky and J. Rzayev, *Macromolecules*, 2016, **49**, 3733-3738.
29 G. Xie, M. R. Martinez, W. F. M. Daniel, A. N. Keith, T. G. Ribelli, M. Fantin, S. S. Sheiko and K. Matyjaszewski, *Macromolecules*, 2018, **51**, 6218-6225.
30 M. Zhong and K. Matyjaszewski, *Macromolecules*, 2011, **44**, 2668-2677.
31 P. J. M. Stals, Y. Li, J. Burdyńska, R. Nicolaÿ, A. Nese, A. R. A. Palmans, E. W. Meijer, K. Matyjaszewski and S. S. Sheiko, *J. Am. Chem. Soc.*, 2013, **135**, 11421-11424.
32 S. S. Sheiko, F. C. Sun, A. Randall, D. Shirvanyants, M. Rubinstein, H.-i. Lee and K. Matyjaszewski, *Nature*, 2006, **440**, 191.